Electronic Supplementary Information

Stencil-printed electrodes without current collectors and inactive additives on textiles for in-plane microsupercapacitors

Xudong Xie,[a,b] Ruisheng Guo,*[a] Bingjun Yang,[c] Haodong Li,[a] Fangshe Yang [b,d] and Baoshou Shen*[b,d]

[a]State Key Laboratory of Solidification Processing, Center of Advanced Lubrication and Seal Materials, School of Materials Science and Engineering, Northwestern Polytechnical University, Xi'an, Shanxi 710072, China

[b]Shaanxi Key Laboratory of Earth Surface System and Environmental Carrying Capacity, Northwest University, Xi'an 710127, China.

[c]Laboratory of Clean Energy Chemistry and Materials, State Key Laboratory of Solid Lubrication, Lanzhou Institute of Chemical Physics, Chinese Academy of Sciences, Lanzhou, 730000, China.

[d]College of Urban and Environmental Sciences/Institute of Earth Surface System and Hazards, Northwest University, Xi'an 710127, China

Keywords: flexible supercapacitors, flexible and printed electronics, wearable electronics, PEDOT:PSS, printable electrodes

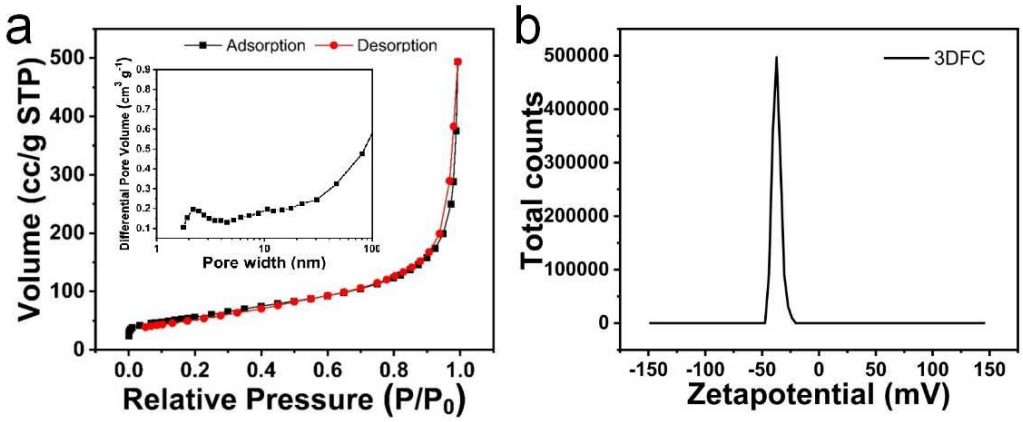

Fig. S1 a) Nitrogen adsorption-desorption curve and pore size distribution (inset) of 3DFC, b) Zeta potential of 3DFC.

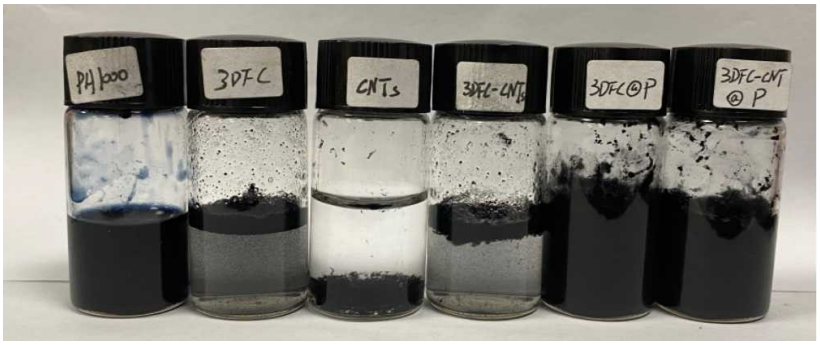

Fig. S2 Digital images of mixtures with different components, including PEDOT:PSS aqueous solution (PH1000), 3DFC in water, CNTs in water, 3DFC-CNTs in water, 3DFC@P aqueous paste, and 3DFC-CNT@P aqueous paste.

Fig. S3 Digital image of 3DFC@P pattern stencil-printed by mask with finger width of 500 μm and finger spacing of 500 μm.

Table S1 Mass loading of each component in different printed electrodes.

	3DFC ($mg \cdot cm^{-2}$)	**CNTs** ($mg \cdot cm^{-2}$)	**PEDOT:PSS** ($mg \cdot cm^{-2}$)	**Mass per unit area** ($mg \cdot cm^{-2}$)	**Total mass** (mg)
3DFC@P IMSC	0.41	0	0.10	0.51	0.655
3DFC-CNT@P IMSC	0.44	0.15	0.15	0.74	0.681

Fig. S4 Digital image of 3DFC@P electrode on cotton showing the bending state at bending angle of 70°.

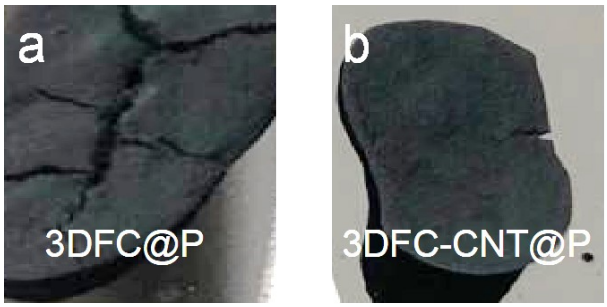

Fig. S5 Digital images of 0.2 ml a) 3DFC@P paste and b) 3DFC-CNT@P paste dropping on silicon wafer after drying.

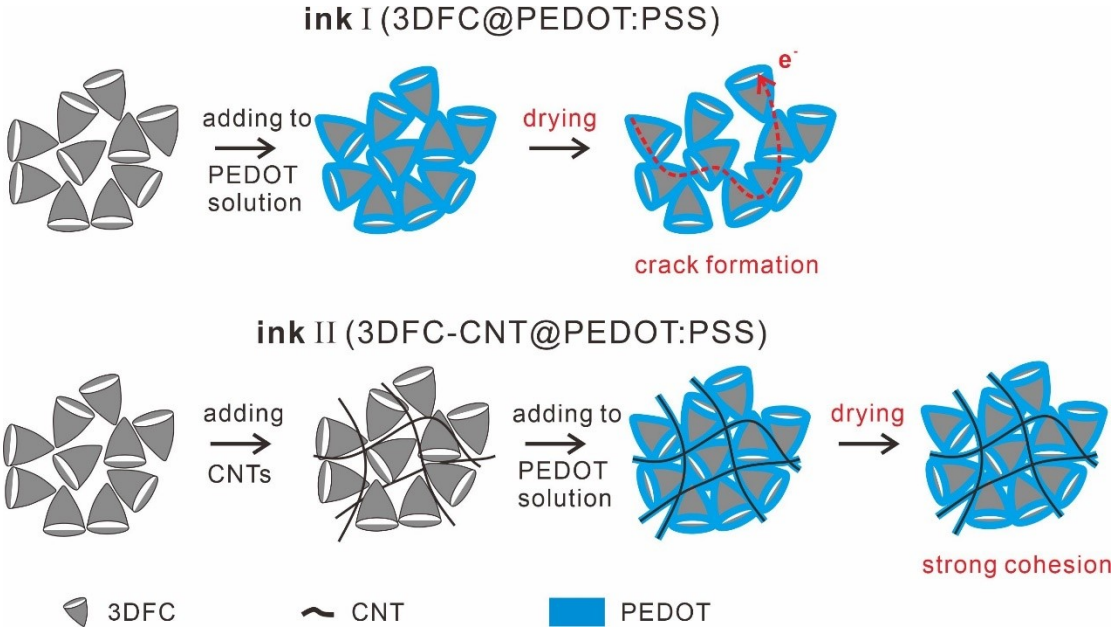

Fig. S6 Scheme of mechanism illustration on decreasing resistance of 3DFC-CNT@P as compared with 3DFC@P.

Cracking of the thick electrode during preparation is a severe issue, which is caused by the uneven shrinkage rates of the electrode in the drying process.[1] In fact, it can also be seen from the respective optical images of both pastes coated on a silicon wafer after drying in **Fig. S5**, the 3DFC@P paste without CNTs have more large cracks than 3DFC-CNT@P, which indicates that the introduction of CNTs with 5~30 μm links the half-eggshell shaped 3DFC and increases the cohesion of 3DFC by PEDOT:PSS binder. Obviously, ink I (3DFC@P) and ink II (3DFC-CNT@P) display different aggregation states. In the electrode composites, from the view of building electrode framework, 3DFC plays the role of skeleton, PEDOT:PSS functions as a binder, and CNTs can act as cross-linkers, respectively. **Fig. S6** gives the detailed mechanism illustration of forming conductive paths for both electrode composites with and without CNTs. For ink I, the large cracks are easily formed after drying which results in less paths of electron transportation. For ink II, in sharp contrast, there are small and less cracks after drying because CNTs bridge the half-eggshell shaped 3DFC, leading to the formation of crosslinked network and spreads of electron paths in all parts. Therefore, 3DFC-CNT@P electrode has lower resistance compared with 3DFC@P electrode.

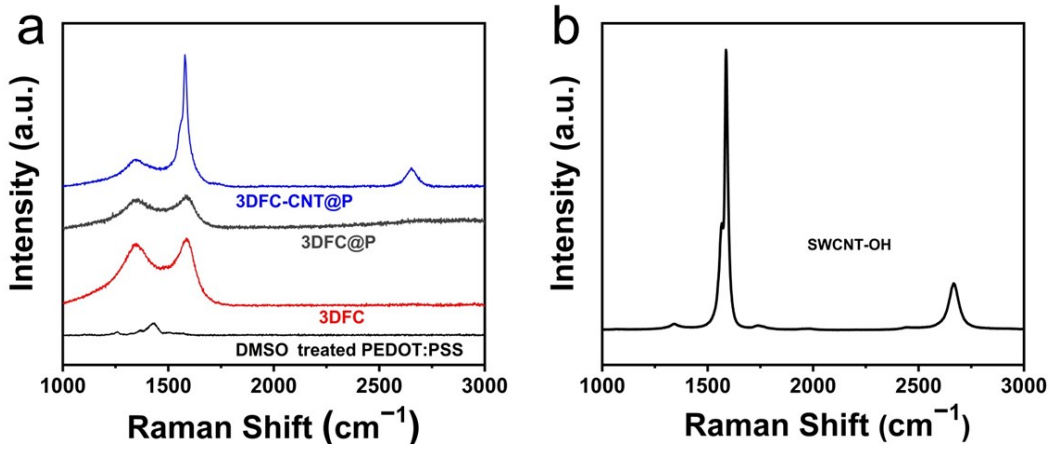

Fig. S7 a) Raman spectrums of the composite and single component of 3DFC-CNT@P paste, 3DFC@P, 3DFC, and DMSO treated PEDOT:PSS. b) Raman spectrum of the CNTs.

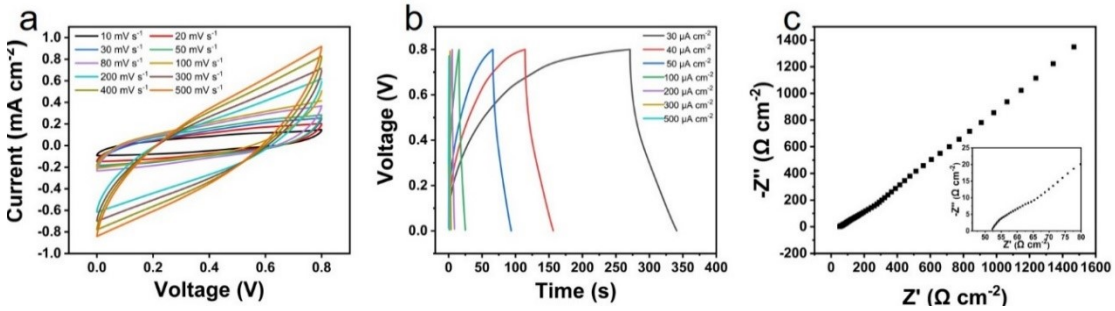

Fig. S8 a) CV curves of 3DFC@P IMSC at different scan rates (from 10 to 500 mV·s^{-1}) with a voltage window of 0-0.8 V, b) GCD profiles of 3DFC@P IMSC at different current density (from 30 to 500 μA·cm^{-2}), c) Nyquist impedance plot in the frequency ranging from 100 kHz to 0.01 Hz of 3DFC@P IMSC with the inset of magnified view.

References:

[1] He, M.; Li, Y.; Liu, S.; Guo, R.; Ma, Y.; Xie, J.; Huo, H.; Cheng, X.; Yin, G.; Zuo, P. Facile carbon fiber-sewed high areal density electrode for lithium sulfur batteries. *Chemical Communications* **2020,** *56* (73), 10758-10761.